Detection and Classification of Material Attributes - A Practical Application of Wavelet Analysis

Peter Maaß[1], Gerd Teschke[1]
Werner Willmann[2], Günter Wollmann[2]

Abstract— **In this paper we describe a method for classifying material properties from measurements of the Barkhausen effect, which originates from a fast magnetization of ferromagnetic materials using alternating currents. We use wavelet analysis to develop a tool box for evaluating Barkhausen measurements. The described wavelet techniques allow to detect extremely weak signals in the Barkhausen noise voltage. By using a statistical classification rule we show that the detected structures are directly related to material properties.**

Keywords— **Material classification, Barkhausen effect, Multiscale decomposition, Wavelet indicator functions, Regression, Discrimination.**

I. Introduction

The increasing automation of manufacturing processes requires new and efficient measuring/testing techniques, which allow to monitor informations about the production process respectively the manufacturing product. Advanced micro electronics, which allows to measure the Barkhausen effect efficiently, combined with mathematical methods from statistical signal analysis allows to evaluate physical effects, which could not be utilized efficiently before.

In this paper we exploit the information contained in measurements of the Barkhausen effect. This effect includes the movements of so-called Bloch-walls in ferromagnetic and poly-crystalline materials. These movements induce some kind of noise voltage. Basic investigations in [22] conjecture and analyze the interdependence of noise voltage and material structures. Hence analyzing measurements of the Barkhausen noise voltage should allow to classify and identify material properties. However using Fourier techniques to analyze the frequency spectrum of Barkhausen noise presents some difficulties. The frequencies are almost uniformly distributed, so far no Fourier-based method allowed to split the measured signal into noise and trend function.

However, using a multiscale decomposition instead of a frequency decomposition exhibits significant structures. The aim of this paper is to justify the use of wavelet analysis for analyzing the Barkhausen effect. Introductory material to the application of wavelet methods in signal processing can be found e.g. in [6][9][13][16][18].

More precisely, we aim at classifying the drawing quality of steel wires. The quality of steel wires depends on the hardening phase during the manufacturing process. The wires may be either not sufficiently hardened (group G_1), properly hardened (group G_2) or not hardened at all (group G_3). The Most important quality parameters are "y_e" (formation of neck in %) and "y_f" (hardness in N/mm^2). The proposed classification scheme for a given piece of wire consists of three steps:

1. The wire is subjected to a periodized magnetization current, the resulting Barkhausen noise voltage u_{BHN} is measured. A typical measurement is displayed in Figure 2,
2. Estimates for y_e and y_f are obtained from the measurements using wavelet methods and a linear regression model,
3. The quality of the wire is classified based on the estimated values $\hat{y}_e$ and $\hat{y}_f$.

The paper is organized as follows: First, for a better understanding, some physical foundations of the Barkhausen noise and a short description of our measuring equipment are given. The second section contains a brief introduction to wavelet analysis. We describe a set of so-called wavelet indicators for analyzing Barkhausen measurements. These indicators are used to determine standard material parameters. Finally, a classification model is used to realize an objective assignment to groups of different material quality.

II. Physical Foundations and Measuring Techniques for the Application of Barkhausen Noise

A. Physical Foundations

The micro structure of ferromagnetic materials consists of magnetic domains with uniform magnetization direction. The direction of the magnetization vectors is statistically distributed in the no-magnetized state. The boundaries between domains of different magnetization are built by thin domain walls inverting the magnetizing direction. Subjected to an external magnetic field these magnetizing vector turn more and more in the direction of this field. This is accompanied by a movement of the domain walls. On reaching magnetic saturation all magnetizing vectors have the same direction and the domain walls disappear. The fine structure of the hysteresis loop $B = f(H)$ of a ferromagnetic sample shows irregular steps (Figure 1) initiated by irreversible movements of the domain walls. The movements cause sudden changes of the magnetic flux, detectable by a sensor coil as induced voltage impulses, the so-called Barkhausen jumps. These jumps can be induced by an external magnetic field (magnetic Barkhausen effect), by mechanical strain of the material (mechanical Barkhausen effect) or by changing temperature. For physical research

[1] Zentrum für Technomathematik, Postfach 33 04 40, Universität Bremen, D-28334 Bremen, Phone: +49 421 218 9497, Fax: +49 421 218 9592, email: pmaass@math.uni-bremen.de, teschke@math.uni-bremen.de

[2] Institut für Elektrotechnik, Technische Universität Bergakademie Freiberg, D-09596 Freiberg

the voltage impulses can be analyzed by nuclear counting techniques. To avoid impulse overlaying very slow magnetization has to be applied.

In contrast to that, fast magnetization with alternating current, e.g. with 50 Hz, produces a noise voltage by a random overlay of all impulses. The continuous frequency spectrum of this measurement ranges from extremely low to high frequencies over 100 kHz. The typical time function of a Barkhausen noise voltage and the magnetizing current is shown in Figure 2. The noise impulse maximum is located close to the zero-magnetic moment of the magnetic field.

B. Influence of Material Properties on the Barkhausen Effect

The fundamental investigations in [22] demonstrated that material properties are reflected in characteristic changes of the noise voltage. The reason is the dependence of domain wall movements in the ferromagnetic materials on features like conductivity, structure (see [21],[7]), fatigue (see [4]), hardness (see [7]), internal and external strain (see [3]), inclusions and so on. This allows to use the Barkhausen effect for non-destructive testing.

With current measurement techniques it is possible to get informations about some material properties by analyzing root-mean-square techniques, envelope curves (see [22],[21]), Fourier spectra (see [3]) or density of amplitudes (see [3]). The problem is, that these results have a rather limited range of applicability: the dependence of material characteristics on the computed indicators can only be shown in some very special cases. Current research aims are finding general relations between material characteristics and the parameters of the Barkhausen voltage.

C. Measuring Equipment

Figure 3 shows the equipment used to measure the Barkhausen noise, including the sensor coil and the magnetization coil enclosing the sample. The magnetization current is produced by a generator with a subsequent power amplifier. The current ranges between 1 mA and 250 mA, the frequency ranges between 1 Hz and 120 Hz. The Barkhausen noise voltage induced in the sensor coil is amplified, filtered and digitized. The frequency characteristic of the amplifier ranges between 10 kHz and 100 kHz. The noise voltage is sampled at 200 kHz and digitized by a 12-bit analogue-to-digital converter. A personal computer controls the measuring process, records the data and synchronizes the magnetizing current with the A/D converter for the noise voltage. The analysis of the noise voltage is realized by a PC or by any other computer equipment.

III. Wavelet Analysis

Over the last decade wavelet methods have developed into powerful tools for a wide range of applications in signal and image processing. The diversity of wavelet methods, however, requires a detailed mathematical analysis of the underlying physical or technical problem in order to take full advantage of this new tool box. This section aims at developing a guideline on how to select an appropriate wavelet and how to interpretate the resulting wavelet transform data for our specific application.

A. Theory

The continuous wavelet transform was introduced in order to overcome the limited time–frequency localization properties of Fourier methods for non–stationary signals. Many papers have been written on the differences and similarities between Fourier and wavelet transform, for detailed information on this topic see e.g. [9],[6] and [16].The wavelet transform correlates the signal f with a shifted and translated test function ψ, $(a, b \in \mathbb{R}, a \neq 0)$:

$$W_\psi f(a,b) \;=\; |a|^{-1/2} \int\limits_{\mathbb{R}} f(t)\overline{\psi\left(\frac{t-b}{a}\right)}\, dt \quad . \qquad (1)$$

The parameter a determines the scale (or size of details) which is examined, the scale becomes finer and finer as a approaches 0. This property has lead to the interpretation of the wavelet transform as a mathematical microscope. It makes sense to consider the transform (1) only if ψ satisfies the following admissibility condition

$$0 < c_\psi := 2\pi \int\limits_{\mathbb{R}} \frac{|\hat{\psi}(\omega)|^2}{|\omega|} d\omega < \infty. \qquad (2)$$

In this case ψ is called a wavelet and the transform (1) is invertible. Some standard examples for wavelets are:

- Haar wavelet $\psi(t) = \begin{cases} 0 & \text{for } t<0 \text{ or } t \geq 1 \\ 1 & \text{for } 0 \leq t < 1/2 \\ -1 & \text{for } 1/2 \leq t < 1 \end{cases}$,
- Mexican hat wavelet $\psi(t) = -\frac{d^2}{dt^2} e^{-t^2/2} = (1-t^2)e^{-t^2/2}$,
- Morlet wavelet $\psi(t) = \pi^{-1/4}\left(e^{-i\ell t} - e^{-\ell^2/2}\right) e^{-t^2/2}$, this wavelet is parameterized by ℓ whose optimal choice depends on the application.
- a complex valued wavelet, which allows a subtle analysis of the phase of the resulting wavelet transform, is the Cauchy wavelet

$$\psi(t) = \Gamma(n+1)(1-it)^{-(n+1)}/2\pi,$$

where Γ is the usual Gamma function (see [2], [13] and Figure 4).

Most applications in signal processing require more than a visual inspection of the wavelet transform. Therefore we need some additional tools for interpreting the computed wavelet transform. Before we start with a list of wavelet tools or wavelet indicators, which are suitable for the problem described above, let us make a more general remark.

Before beginning to analyze any signal with wavelet methods one should answer three basic questions:

- Why should wavelet analysis help to solve this specific problem?
- Which wavelet should be used?
- Which tools for interpretating the computed wavelet transform will reveal the desired information?

The first question can be answered positively whenever the signal has some multiscale structure or if the searched

for information lives on an a priori unknown scale. Our problem of evaluating a signal with no apparent structure falls in this second class of problems: the searched for information is contained in details/structures of yet unknown size and shape. The wavelet transform allows, due to its bandpass filtering property, to scan the signal on different frequency bands or detail scales simultaneously. In the case of Barkhausen noise we suppose that the scales between the noise and the background oscillation imposed by the magnetization current contain the desired information.

The answer to the second question usually requires to study the physical/mathematical background of the problem at hand. Since there does not exist a mathematical model, which reflects the influence of the desired material properties on the Barkhausen measurements, we choose a "general purpose" wavelet which allows a detailed analysis of amplitude and phase, i.e. a Cauchy wavelet.

This choice can be further justified by the following argument: Wavelets of high regularity and excellent time-scale localization properties are preferable. First, we wish to quantify the localization properties of wavelet transforms. This is measured by the uncertainty principle of the affine group, which is minimized by functions of the following type (for details see [8]):

$$\varphi(t) = c(t-\lambda)^{\alpha}. \tag{3}$$

Using $\lambda = -i$, $\alpha = -2$ and $c = -\sqrt{2/\pi}$ we obtain the set of normed Cauchy wavelets (Figure 4) as minimizers of the affine uncertainty principle (see [20]). To establish a analytical interpretation of the wavelet transform we have to look how the Cauchy wavelets are constructed (see [13]). They are derivatives of the Cauchy kernel

$$\psi_{c,n}(t) = d^n/(i^n dt^n)C(t) = \frac{1}{2\pi}\Gamma(n+1)(1-it)^{-(n+1)}, \tag{4}$$

where the kernel $C(t)$ is equal to $(2\pi(1-it))^{-1}$. These wavelets are of high regularity. This is obvious because of the fast decrease of its Fourier transform. Further the Fourier transform is real valued and progressive. In case of having a real signal f (indeed the used Barkhausen measurements are real) the analysis with a Cauchy wavelet means consequently no a priori loss of informations (every real function may be recovered from it's progressive part). Further, for analytical interpretation, we remark that the wavelet transform with respect to Cauchy wavelets is related to the analysis of analytic functions over the complex half-plane (see [5], [13], for detailed calculation [20] and [23]). Since the Cauchy wavelets include both, excellent analytical and localization attributes, our numerical realizations were computed with one of them (Figure 5, for simplicity we prefer $n = 1$). A more detailed description of complex valued wavelet transforms and their application in signal processing can be found e.g. in [1], [12], [17] and [20].

B. Choice of Wavelet Indicators

In this section we want to answer the last question, the most difficult one. We list some interpretation tools or indicators for our specific problem. Following the above theory, a solution to our problem now consists in constructing an adequate finite choice of indicators ϑ_n, which depend on phase and/or modulus of the calculated complex wavelet transforms (using Cauchy wavelets). Finally a relation between the material parameters (G_1, G_2 and G_3) and the computed indicators has to be determined.

First we turn to the introduction of indicator functions based on the computed wavelet transforms. The indicators should allow to distinguish between different materials. Since we do not have a mathematical model which relates our data to the desired material properties we have to search for and experiment with a general family of indicators. These indicators are then used as input data for a statistical classification process. The classification is based on a regression model, see below.

Extensive test computations revealed no significance of the computed phase representations. Hence the phase information is not used in the subsequent analysis, which is entirely based on the modulus of the wavelet transform. Let $W_{\psi_c}u_{BHN}(a,b)$ denote the wavelet transform of the Barkhausen data u_{BHN} with respect to a Cauchy wavelet ψ_c, then its squared L^2–norm with respect to the scale parameter is

$$\Psi(b) = \int |W_{\psi_c}u_{BHN}(a,b)|^2 da\ . \tag{5}$$

The function Ψ can also be interpreted as the second moment of $|W_{\psi_c}u_{BHN}(a,b)|$ with respect to the left invariant Haar measure $\frac{da}{a^2}$. The shapes of Ψ for different type of steel wires are shown in Figure 6. By exploring the modulus we can determine some so-called wavelet indicators as follows:

- $\vartheta_1 = b_0$ with $\Psi(b_0) \geq \Psi(b)$, $\forall\ b \neq b_0$, this indicates the position of the maximum and
- $\vartheta_2 = \Psi(\vartheta_1)$ the value of maximum of Ψ.
- $\vartheta_3 = \int\limits_{b\leq b_0} \Psi(b)db$ and $\vartheta_4 = \int\limits_{b>b_0} \Psi(b)db$ reflect how the weight of the integral is distributed.

If we suppose that $\tilde{\Psi} = \Psi/(\vartheta_3+\vartheta_4)$ represents relative frequencies (Figure 6) in a statistical sense, then $\tilde{\Psi}$ can be interpreted as a density function of any empirical distribution. Using this motivation one can fix the expectation of $\tilde{\Psi}$:

- $\vartheta_5 = \int b\tilde{\Psi}(b)db$.

Next, we consider the kth empirical moment m_k of $\tilde{\Psi}$, which leads to the statistical values skewness and excess: Using common definitions we define the indicators

- $\vartheta_6 = \frac{m_3}{(m_2)^{3/2}}$ (=skewness) and
- $\vartheta_7 = \frac{m_4}{(m_2)^2} - 3$ (=excess).

These seven indicators were chosen empirically based on extensive computations and general experience with similar signal processing applications.

IV. Classification Model and Numerical Results

In this section we establish a relation between the seven wavelet indicators $\vartheta_1, .., \vartheta_7$ and the material parameters y_e and y_f. Therefore we introduce a linear regression model. Finally, a maximum likelihood classification rule is used in order to classify the type of steel wires according to the estimated values $\hat{y}_e$ and $\hat{y}_f$.

A. Regression

The linear regression model (see [14]) is based on fifteen samples of noise voltage u_{BHN}, with known vectors Y_e and Y_f. The linear models for Y_e and Y_f are of the following type:

$$Y_e = \Theta\beta^e + \varepsilon_e \quad \text{and} \quad Y_f = \Theta\beta^f + \varepsilon_f \ , \tag{6}$$

where $\Theta = (\mathbf{1}, \theta_1, \ldots, \theta_7)$ and $\mathbf{1} = (1, \ldots, 1)^T$, $\theta_1 = (\vartheta_1^1, \ldots, \vartheta_1^{15})^T$, $\theta_2 = (\vartheta_2^1, \ldots, \vartheta_2^{15})^T$, ... denote the indicator values for the different test samples. The error terms ε_e and ε_f are random variables with $\mathsf{E}\varepsilon_e = 0$, $\mathsf{Var}\varepsilon_e = \sigma_e^2 W_e$ and $\mathsf{E}\varepsilon_f = 0$, $\mathsf{Var}\varepsilon_f = \sigma_f^2 W_f$, where W_e and W_f are positive definite.

We use the method of least squares, which yields best linear unbiased estimators $\hat{\beta}$ for β. Therefore we have to minimize two sums $\|Y_e - \Theta\beta^e\|^2_{W_e^{-1}}$ and $\|Y_f - \Theta\beta^f\|^2_{W_f^{-1}}$. If the matrix Θ has full rank then $\Theta^T\Theta$ is regular and the estimations

$$\hat{\beta}^f = (\Theta^T W_f^{-1}\Theta)^{-1}\Theta^T W_f^{-1} Y_f \quad \text{and}$$

$$\hat{\beta}^e = (\Theta^T W_e^{-1}\Theta)^{-1}\Theta^T W_e^{-1} Y_e$$

are the unique minimizers (see [14]). The regularity of $\Theta^T\Theta$ has been checked numerically in our case. The resulting estimates for β^e and β^f are shown in Table 1.

We may check the quality of this linear model by using the estimated parameter vectors $\hat{\beta}^e$ and $\hat{\beta}^f$ to recover the vectors $\hat{Y}_f$ and $\hat{Y}_e$. The norms $\|Y_e - \hat{Y}_e\| = 7.340 \cdot 10^{-07}$ and $\|Y_f - \hat{Y}_f\| = 2.151 \cdot 10^{-05}$ can be interpreted as the variances of the errors in (6). The errors are small but in order to have an objective group assignment of some unknown samples we will introduce a simple model for classification in the next section.

B. Discrimination

As exemplified above, the last step is to classify a sample u_{BHN} as a member of G_1, G_2 or G_3. An elementary tool for attaining this is the maximum likelihood classification rule. We begin with some basic considerations. Assume we have three distributions P_{ν_1}, P_{ν_2} and P_{ν_3} which characterize G_1, G_2 and G_3 and three related two-dimensional random variables X_1, X_2 and X_3: $X_1 \sim P_{\nu_1}$, $X_2 \sim P_{\nu_2}$ and $X_3 \sim P_{\nu_3}$. Now, starting with an estimated vector $\hat{y} = (\hat{y}_e, \hat{y}_f)^T$ of a sample u_{BHN} we like to check whether $\hat{y}$ is a realization of a distribution similar to X_1, X_2 or X_3.

We want to be a bit more general. Let us consider a family of distributions P_ν parameterized by a parameter space Δ. Moreover, let us assume for a moment that we know the distributions P_{ν_1}, P_{ν_2} and P_{ν_3}, where P_{ν_i} describes the distribution of $y \in \mathbb{R}^2$ for the different types G_1, G_2, G_3. Let p_{ν_i} denote the corresponding density functions. Then we can define sets in $\mathbb{R}^2$ by $A_i = \{y : \ p_{\nu_i}(y) = \max_j p_{\nu_j}(y)\}$. One A_i includes those arguments y where $p_{\nu_i}(y)$ is maximal. A data sample is then classified by the computed vector $(\hat{y}_e, \hat{y}_f)$ according to its position $(\hat{y}_e, \hat{y}_f) \in A_{i^*}$, (see [10],[11],[14]).

However we don't know P_{ν_1}, P_{ν_2} and P_{ν_3}. Hence we first have to estimate ν_1, ν_2, ν_3, where we assume that the distributions P_ν are parameterized by a parameter space Δ. Since we don't know a better model we require independent and normal distributed variables. Hence we can estimate the unknown parameters of the three two-dimensional normal distributions $P_{\nu_i} = \mathsf{N}_2(\mu_i, \Sigma_i)$, where $\nu_i = (\mu_i, \Sigma_i)$. With the given observations we can determine μ_i and Σ_i by using the maximum likelihood estimators of μ_i and Σ_i, see [14],[15]. Note that we have 5 known samples for each group G_i:

$$\hat{\mu}_i = \frac{1}{n}\sum_{j=5i-4}^{5i} y_j \text{ and } \hat{\Sigma}_i = \frac{1}{n}\sum_{j=5i-4}^{5i} (y_j - \hat{\mu}_i)(y_j - \hat{\mu}_i)^T,$$

where y_j is computed to u^j_{BHN}. We get $\hat{\nu}_i$ for ν_i and thus distributions $\mathsf{N}_2(\hat{\mu}_i, \hat{\Sigma}_i)$. Now we may define the classification rule: *From the given data u_{BHN} we compute $z = (\hat{y}_e, \hat{y}_f)$ using the linear regression model described in the previous section. Then u_{BHN} belongs to group G_i if*

$$(z - \hat{\mu}_i)^T \hat{\Sigma}_i^{-1}(z - \hat{\mu}_i) < (z - \hat{\mu}_j)^T \hat{\Sigma}_j^{-1}(z - \hat{\mu}_j) \quad \forall i \neq j \quad .$$

C. Evaluation of unknown samples

Nine unknown samples were analyzed. For the estimated values $\hat{y}_e$ and $\hat{y}_f$ see Table II. Further Table II shows the realized classifications. Figure 7 displays the three connected domains of classification A_1 , A_2 and A_3. Since the variances differ, $\hat{\Sigma}_i \neq \hat{\Sigma}_j$ for $i \neq j$, we have quadratic separating functions instead of linear ones. An subsequent inspection showed that $\hat{y}_5$, resp. $\hat{y}_7$ were assigned incorrectly. The correct classifications G_1, resp. G_2. The essential reason of misclassification is the very weak material dependent structure in Barkhausen noise voltage. And the appearance of misclassifications only in a small neighborhood of the boundary between G_1 and G_2 indicates the quality of the model.

V. Summary

By using wavelet analysis combined with statistical methods we developed a method for classifying the quality of ferromagnetic materials. The success of the method demonstrates the existence of a relation between Barkhausen noise voltage and material parameters.

Precisely, we have introduced a new method to utilize Barkhausen noise for testing the drawing quality of wires. For that purpose wire samples were selected with the same composition but different strength factors (hardness) caused by different annealing times. The strength factors were determined by non-destructive material testing.

First, the data samples were analyzed by complex wavelet transforms with respect to Cauchy wavelets. After constructing a set of significant indicators we used linear regression to relate these to material parameters. To realize an objective assignment the classical maximum likelihood classification rule was used.

After this calibration process, the resulting classification scheme was used for analyzing nine different, a priorly unknown data sets. Seven data sets were classified correctly,

but two of the test samples u^j_{test} were assigned incorrectly, they correspond to the classification results close to the boundary between G_1 and G_2, see Figure 7.

References

[1] A. Aldroubi, M. Unser: *WAVELETS in Medicine and Biology*. CRC Press, 1996.

[2] J.-P. Antoine, R. Murenzi, P. Vandergheynst, Directional wavelets revisited: *Cauchy wavelets and symmetry detection in patters*, Appl. Comput. Harmon. Anal. **6** (1999) 314-345.

[3] D.-L. Atherton, L. Clapham, C. Jagadish: *Influence of Uniaxial Elastic Stress on Power Spectrum and Pulse Height Distribution of Surface Barkhausen Noise in Pipeline Steel*. IEEE Transactions on Magnetics, Volume 26 (1990), No. 3 p.1160-1163

[4] C. Blochwitz, C. Buque, W. Tirschler: *Barkhausenrauschen in mechanisch ermüdeten Nickelkristalen*. Zeitschrift Metallkunde 86, S. 1-12, (1995).

[5] R. Busam, E. Freitag: *Funktionentheorie*. Springer Verlag, Berlin, 1993.

[6] Ch.K. Chui: *An Introduction to WAVELETS*. Academic Press, San Diego, 1992.

[7] A. Cowking, R. S. Geng, R. Hill, J. W. Mackersie: *The effect of nickel hardness and grain size on acoustic and electromagnetic Barkhausen emission*. NDT&E International, Volume 24 (1991), No. 4 p.179-186

[8] S. Dahlke, P. Maaß: *The Affine Uncertainty Principle in One and Two Dimensions*. Comp. Math. Appl. vol. 30, No. 3–6, S. 293–305 (1995).

[9] I. Daubechies: *Ten Lectures on Wavelets*. Society for Industrial and Applied Mathematics (SIAM), Philadelphia, 1992.

[10] J. Devore, R. Peck: *Statistics*. Belmont, 1993.

[11] M. Fisz: *Wahrscheinlichkeitsrechnung und Mathematische Statistik*. Berlin, 1989.

[12] A. Grossmann, R. Kronland-Martinet, J. Morlet: *Reading and understanding continuous wavelet transform*. In: Wavelets: Time-Frequency Methods and Phase Space, Inverse Problems and Theoretical Imaging, Springer Verlag, 1989.

[13] M. Holscheider: *Wavelets An Analysis Tool*. Clarendon Press, Oxford, 1995.

[14] J.D. Jobson: *Applied Multivariate Data Analysis*. Springer Verlag, 1991.

[15] T. Katsuto: *Time Series Analysis*. Wiley-Interscience Publication, New York, 1996.

[16] A.K. Louis, P. Maaß, A. Rieder: *Wavelets*. Teubner, Stuttgart, 1994.

[17] P. Maaß : *Wavelet Methods and Applications in Signal Processing*. in "Advanced Mathematical Methods in Metrology III", Eds. P. Ciarlini, M.G. Cox, F. Pavese, D. Richter World Scientific, Singapur, S. 91 –104 (1997)

[18] S. Mallat: *A Wavelet Tour of Signal Processing*. Academic Press, San Diego, 1998.

[19] Y. Meyer: *Wavelets and Operators*. Cambridge University Press, 1992.

[20] G. Teschke: *Komplexwertige Wavelets und Phaseninformation, Anwendung in der Signalverarbeitung*. Diplomarbeit, Potsdam, 1998.

[21] W. Willmann, G. Wollmann: *Der Barkhausen-Effekt und seine meßtechnische Nutzung*. Experimentelle Technik der Physik 31, S.533-543, (1983).

[22] W. Willmann, G. Wollmann: *Gerätesystem zur Auswertung des Barkhausenrauschens*. Wiss. Beträge der IH Zwickau 11, S. 64-66, (1985).

[23] K. Yosida: *Functional Analysis*. Springer Verlag, 1980

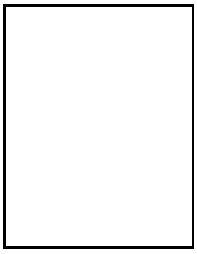

Peter Maaß studied from 1979 to 1985 mathematics at the Technical University Karlsruhe, Germany, and at the Pembroke College in Cambridge (UK). He received the Diploma in mathematics from the University of Heidelberg, Germany, in 1985, the Dr. (PhD) degree from the Technical University Berlin in 1988. From 1990 to 1991 he was assisant professor in Boston at Tufts University and from 1991 to 1993 he was assisant at the University of Saarbrücken where he received in 1993 the Dr. habil. degree. From 1993 to 1999 he was professor of mathematics at the University of Potsdam. Currently he is professor of mathematics at the University of Bremen where he is the director of the Center of Technomathematics.The emphasis of his research is applied functionalanalysis, in particular wavelet analysis and inverse problems. He is in the editorial board of several mathematical journals.

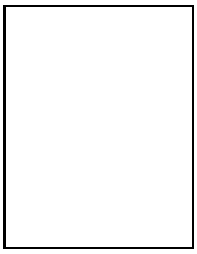

Gerd Teschke studied from 1993 to 1998 mathematics at the University of Potsdam, Germany, and at the Universidade de Coimbra and Aveiro, Portugal. He received the Diploma in mathematics in 1998 from the University of Potsdam. Currently he is PhD-student in the Center of Technomathematics (research team of Prof. P. Maaß) at the University of Bremen. His mathematical field of activities contains wavelet analysis and connected applications.

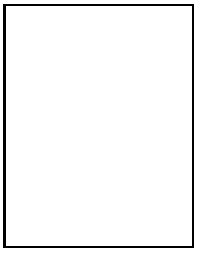

Werner Willmann is the Head of the Department of Electrical Measurement and Sensor Technology on the Institute of Electrical Engineering at the Freiberg University of Mining and Technology in Germany. He received the Dr.-Ing. (PhD) and the Dr.-Ing. habil. degrees from the Freiberg University. His main research fields are the Barkhausen effect and the development of measurement devices.

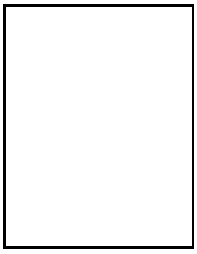

Günter Wollmann received the Dipl.-Ing. (diploma) in Electronic Technology from the Technical University Dresden and the Dr.-Ing. (PhD) degree in Information Technology from the Freiberg University of Mining and Technology. He works as scientific assistent at the Freiberg University and his activities are the development of measurement devices and sonsors as well as the analysis of noise.

Figures and Tables

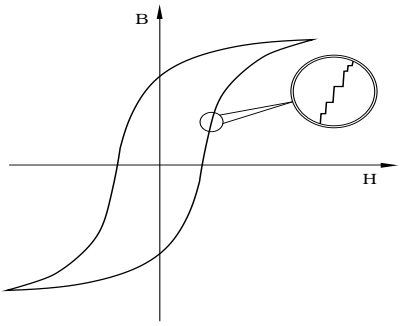

Fig. 1. Hysteresis loop and their microstructure

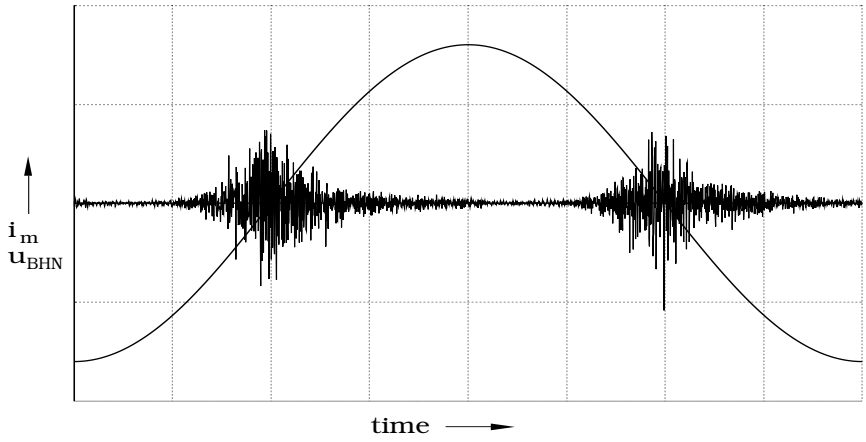

Fig. 2. Barkhausen noise voltage u_{BHN} and magnetizings current i_m against time

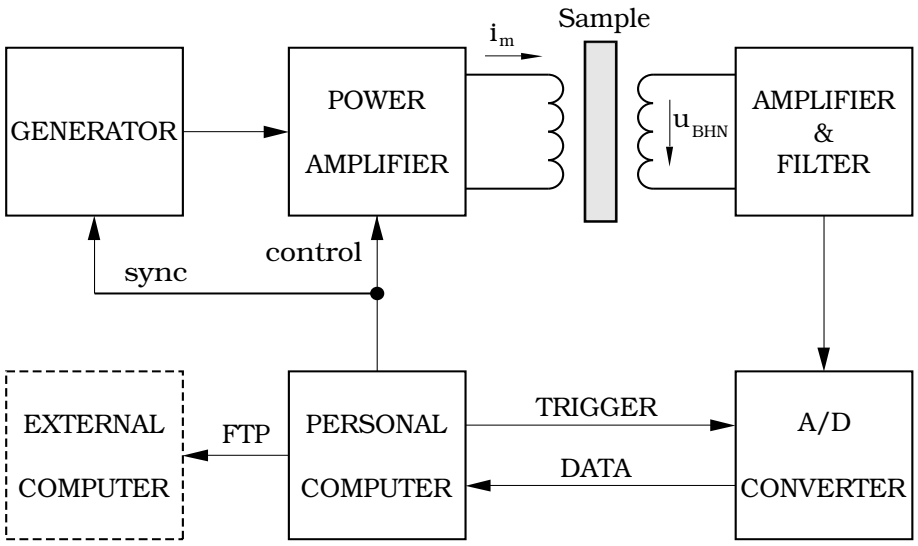

Fig. 3. Scheme of measuring equipment

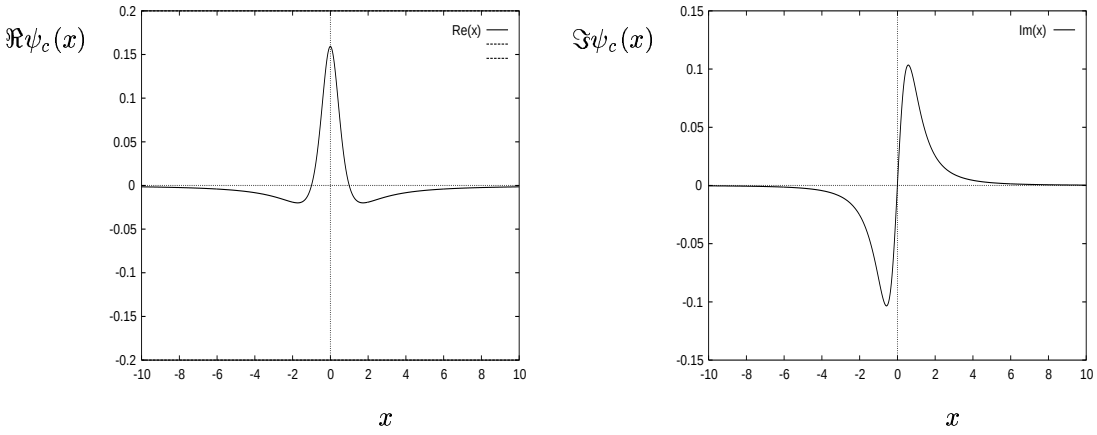

Fig. 4. A Cauchy wavelet for $n = 1$. On the left side the real and on the right side the imaginary part is represented.

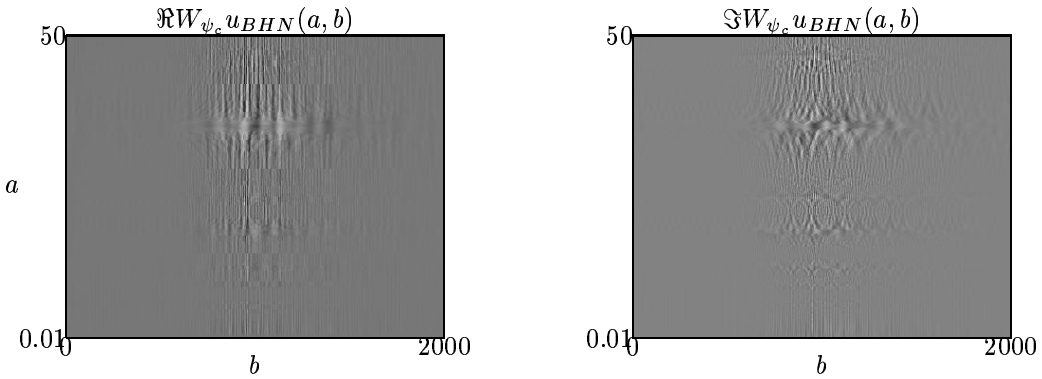

Fig. 5. Visualization of the complex valued wavelet transform of one impulse with respect to a Cauchy wavelet ($n = 1$). On the left side the real and on the right side the imaginary part is represented.

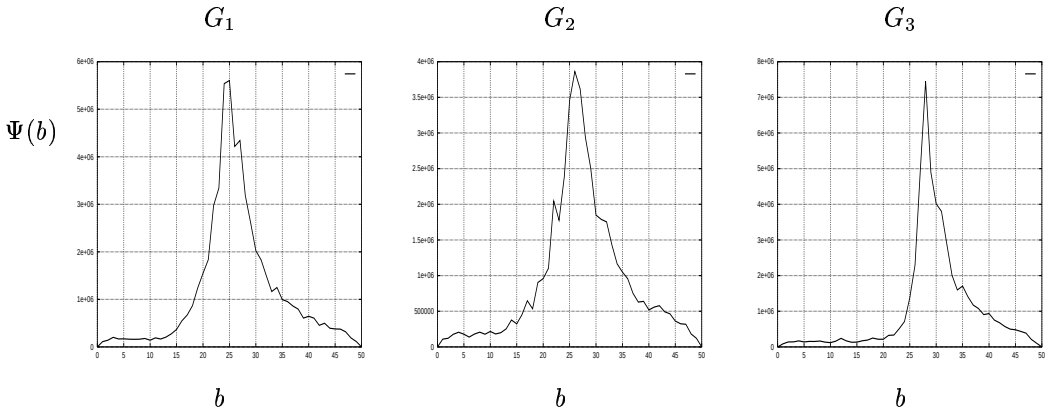

Fig. 6. Representations of Ψ with respect to one member of G_1, G_2 and G_3 (calculated on a grid).

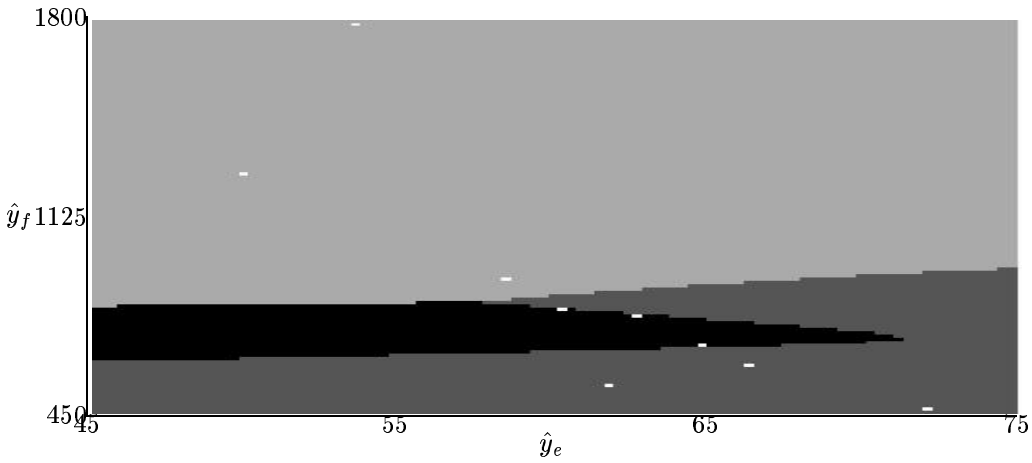

Fig. 7. Classification domains of a nonlinear discrimination of nine concrete test samples. Different colors are representing different groups ($G_1 \sim$ black, $G_2 \sim$ dark gray and $G_3 \sim$ light gray). The white points are recovered values of material parameters.

	y_f	y_e	$\hat{y}_f$	$\hat{y}_e$
G_1	708	64.7	707.9	64.69
G_1	697	62.7	696.9	62.69
G_1	708	67.7	707.9	67.69
G_1	725	61.2	724.9	61.19
G_1	713	65.8	712.9	65.79
G_2	600	67.7	599.9	67.69
G_2	665	67.3	664.9	67.29
G_2	617	66.1	616.9	66.09
G_2	649	70.5	648.9	70.49
G_2	649	70.5	648.9	70.49
G_3	1294	49.0	1293.9	48.99
G_3	1344	53.9	1343.9	53.89
G_3	1400	46.1	1399.9	46.09
G_3	1334	47.2	1333.9	47.19
G_3	1400	56.1	1399.9	56.09

	$\hat{\beta}^f$	$\hat{\beta}^e$
1	$-4.608 \cdot 10^3$	$1.699 \cdot 10^2$
ϑ_1	$-3.855 \cdot 10^2$	$1.821 \cdot 10^1$
ϑ_2	$6.026 \cdot 10^{-5}$	$-2.131 \cdot 10^{-6}$
ϑ_3	$4.219 \cdot 10^{-5}$	$-2.008 \cdot 10^{-6}$
ϑ_4	$-2.007 \cdot 10^{-5}$	$1.167 \cdot 10^{-6}$
ϑ_5	$5.186 \cdot 10^2$	$-1.987 \cdot 10^1$
ϑ_6	$-1.733 \cdot 10^2$	$1.272 \cdot 10^1$
ϑ_7	$1.479 \cdot 10^2$	$-5.973 \cdot 10^0$

TABLE I

THE FIRST TABLE SHOWS THE VALUES OF GIVEN OBERVATIONS Y_f AND Y_e AND THE RECOVERED VECTORS $\hat{Y}_f$ AND $\hat{Y}_e$. THE SECOND TABLE SHOWS THE ESTIMATED MODEL PARAMETERS $\hat{\beta}^f$ AND $\hat{\beta}^e$ FOR THE GIVEN OBSERVATIONS.

j-th test sample	$\hat{y}_e$	$\hat{y}_f$	classification
1	72.01	466.89	G_2
2	58.48	911.48	G_3
3	50.01	1275.54	G_3
4	60.39	809.49	G_1
5	66.19	622.04	G_2
6	53.71	1771.89	G_3
7	64.93	677.36	G_1
8	62.57	807.21	G_1
9	61.94	556.49	G_2

TABLE II

RECOVERED MATERIAL PARAMETERS OF NINE TEST SAMPLES AND THE CLASSIFICATION IS REPRESENTED.